Pattern Recognition Letters 11 (1990) 443–452
North-Holland

June 1990

Pattern recognition techniques in analyzing the effect of thiourea on brain neurosecretory cells

Sankar Kr. PAL

Electronics & Communication Sciences Unit, Indian Statistical Institute, 203 Barrackpore Trunk Road, Calcutta 700035, India

Atanu BHATTACHARYYA

Department of Zoology, Vidyasagar College for Women, Calcutta 700006, India

Received 30 August 1989

Abstract: The effect of thiourea on brain neurosecretory cells has been analysed using pattern recognition and image processing techniques. Preprocessing and primitive extraction are done using fuzzy set theoretic approaches. The syntactic classification of various cellular abnormalities (e.g., normal, initial abnormal, middle abnormal and lethal abnormal), on the other hand, has been achieved using ordinary grammar. An experiment for creating various abnormalities is explained. The pattern variability in terms of dimension is also statistically analysed.

Key words: Neurosecretory cells, thiourea, pattern recognition, fuzzy sets.

1. Introduction

Neurosecretion is a general phenomenon, occurring in all animals, and is nothing but the process of synthesis of hormone (called neurohormone) from the brain neurosecretory cells. Brain neurosecretory cells are located mostly in the first part of the insect brain, called parintercerebralis. One of these cells is called 'A' type which is larger in size, and is prone only to some specific stains such as chrome hematoxylin and paraldehyde fuchsin [1]. The 'A' type cells are also predominant in number. Most of the physiological functions are regulated by these 'A' type cells [1]. The abnormality occurring in these cells, therefore, affects the physiological processes e.g., reproductive and oxidative mechanisms etc. The abnormalities might occur because of pollutants in the environment; thus resulting in various cancerous growth.

The study of abnormalities in the neurosecretory cells therefore becomes necessary in order to make a diagnosis of their cancerous growth. Such an investigation will also facilitate the diagnosis of various abnormalities in the brain neurosecretory cells of man.

The present work is an attempt to analyse the cell abnormalities by a machine using image processing and pattern recognition techniques. In order to do this, the brain cells of *Periplaneta americana* (cockroach) have been considered here, as an example.

The role of insecticides in creating abnormalities in neurosecretory cells of insects has been studied by several authors [3–5]. On the other hand, the role of thiourea in this regard has not been properly investigated. Thiourea is a chemosterilant, i.e., a chemical which sterilises the reproductive processes and inhibits the different biological mechanisms [6–8]. In view of the above fact, thiourea has been considered in our experiment for creating cellular abnormalities. Different concentrations of thiourea were injected in creating such abnormalities. Abnormalities in the brain neurosecretory cells of the cockroach are seen to be reflected in

both the nuclear and cell membrane architecture of these cells.

The pattern recognition techniques involved here, therefore, incorporate the tasks of preprocessing, primitive extraction and classification of different varieties of nuclear and cellular shape patterns. The pre (image) processing operations include enhancement and contour extraction of nuclear and cellular patterns corresponding to normal and abnormal neuron cells. Primitives extracted are namely, arcs (both clockwise and anticlockwise) of different curvature and straight lines obtained from the octal code representation of contours. Each string thus formed corresponding to the shape of an unknown pattern is finally classified using syntactic technique. Both fuzzy and nonfuzzy approaches [9–11] have been considered in the above mentioned operations. Besides these, the pattern variability reflected in their dimension is also shown experimentally. Results of statistical analysis including 't' test of cellular dimension in this context have been discussed.

2. Different stages of neurosecretory cell abnormalities

2.1. Experiment for creating abnormalities

Periplaneta americana were reared in the laboratory at 30 ± 1 °C and fed on bread with water. The female *Periplaneta americana* from the same mother were divided at random into different groups for experiments. Each group consisted of 50 fully matured female cockroaches. Thiourea (Analar, BDH, Glaxo Laboratories, India) was used for treatment. Thiourea of different doses (8 μl, 16 μl and 20 μl/female) were given in a single injection through the 4th abdominal segment. The control adult female cockroaches were injected with an equivalent amount of distilled water and kept side by side with the treated cockroaches.

All fully matured female cockroaches were sacrificed just after three days, i.e., after 72 hours of the injection. The entire brain of the female cockroach was dissected out quickly and employed in Bouin's fixative. In order to study 'A' cells, we employed the following stains: chrome hematoxylin phloxin (CHP), paraldehyde fuchsin (PF), alcian blue, alcian yellow and paraldehyde thionin phloxin (PTh-Ph) using Panov's method. After staining the slides were dehydrated and mounted with DPX.

2.2. Observations

The above experiment revealed that a single injection of thiourea at different concentrations (8 μl, 16 μl and 20 μl/female) not only impairs the structural architecture of 'A' type neurosecretory cells and cell nuclei, it also causes reduction in size (Table 1) and shrinkage of the cells and nuclear membrane (compare Figures 1(b), 1(c) and 1(d) to the normal case, Figure 1(a)). Figure 1(a) shows a normal 'A' type neurosecretory cell. Figure 1(b) illustrates the initial change by a 8 μl/female of thiourea injection when the nuclear membrane and cell membrane become gradually smaller in size. At 16 μl/female injection, more deposition of neurosecretory material occurs inside the cell and the cell size reduces further. This is shown in Figure 1(c). Figure 1(d) is related to 20 μl, a lethal dose, which is associated with massive degradation of the neurosecretory cells. This degradation is due to the inhibition of oxidative phosphorylation and results in different sizes and shapes of nuclear and cellular contours.

Table 1
Effect of thiourea on brain neurosecretory cell size and on nuclear size of neurosecretory cells of *Periplaneta americana*. 8 μl, 16 μl and 20 μl/female of thiourea were injected in cockroach and sacrificed after 72 hrs.

Dose	Median neurosecretory cell size 'A' type Mean ± S.E. (μm)	Nuclear size of the median neurosecretory cells 'A' type Mean ± S.E. (μm)
Control	35.06 ± 0.89	18.83 ± 0.01
8 μl/female	27.19 ± 0.02*	14.57 ± 0.001*
16 μl/female	25.58 ± 0.01*	13.14 ± 0.003*
24 μl/female	24.83 ± 0.003*	11.35 ± 0.29*

S.E. = Standard Error
* denotes $P < 0.001$, P is the value of student 't' test

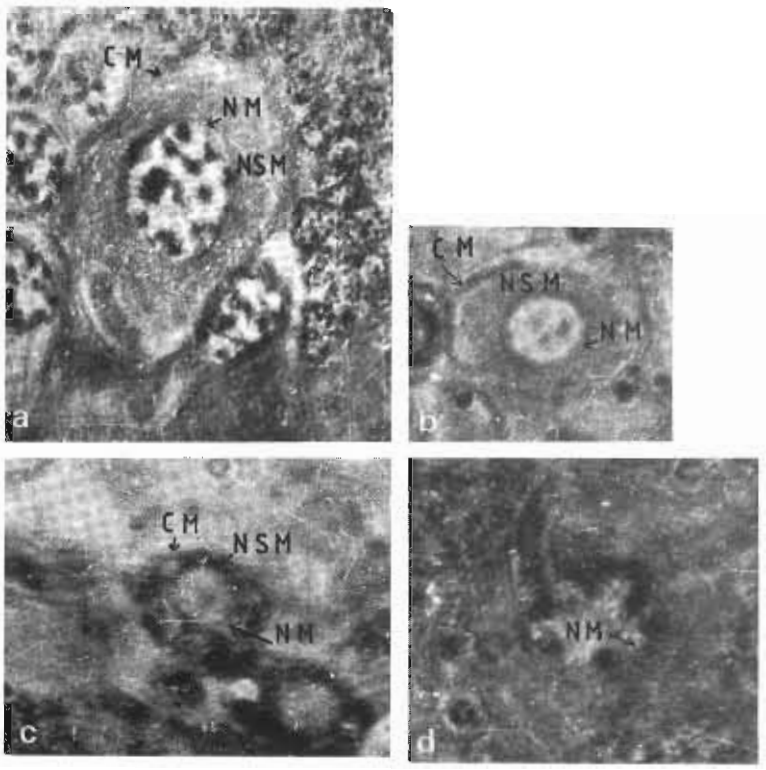

Figure 1. Showing the effect of thiourea on 'A' type neurosecretory cells of Pars Intercerebralis region of brains of *Periplaneta americana*. NM: Nuclear membrane, NSM: Neurosecretory Material, CM: Cell membrane. (a) Normal brain neurosecretory cells [10×100]. (b) Abnormal neurosecretory cells after injection with thiourea, 8 μl/female [10×100]. (c) Abnormal brain neurosecretory cells after injection with thiourea, 16 μl/female [10×100]. (d) Lethal brain neurosecretory cells after injection with thiourea, 20 μl/female [10×100].

The variation in their size is reflected numerically by the figures given in Table 1. Regarding the variation in shape, it is to be pointed out that the shape of the nuclear membrane remains more or less circular after doses of 8 and 16 µl/female are used. This indicates that the change occurs very rarely in the nuclear contour as compared to the cell surface contour, except for the dose of 20 µl when a massive nuclear breakdown makes its shape irregular. In the following sections we shall therefore present algorithms for identifying these various abnormalities in terms of cellular shape patterns only. This together with the discrimination ability based on their dimension will lead us to a final decision on different abnormalities.

3. Recognition algorithms and results

The problem of recognition involves three major parts, namely,

(a) preprocessing of cell images with a view to extract the edges of nuclear and cellular cells,

(b) primitive extraction of the edge detected images, and

(c) syntactic classification into one of the possible stages among normal and abnormalities.

These are explained below.

3.1. Enhancement and edge detection

It is seen from Figure 1 that the boundaries of the cells are ill-defined (fuzzy). The images therefore need contrast enhancement before detecting their contours. There are numerous algorithms available [9,11] using both fuzzy and nonfuzzy techniques to perform this task automatically. Here we have adopted the ones formulated by Pal and King [12] using a contrast intensification (INTR) [13] operator for enhancement and a max-min operation based edge detection [14] procedure.

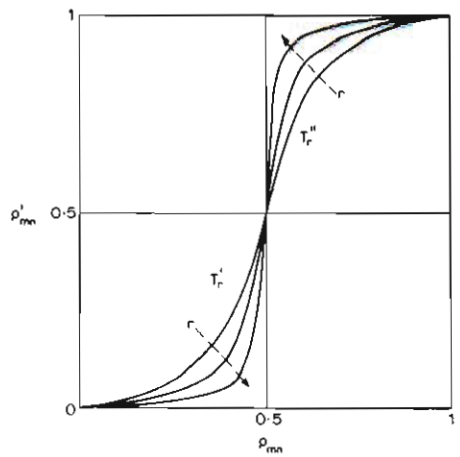

Figure 2. INT transformation function. P_{mn} and P'_{mn} are the original and enhanced property values of x_{mn}.

For the sake of reader's convenience, the INT transformation function for contrast enhancement in fuzzy property domain P_{mn} is shown in Figure 2. It is defined for an $M \times N$ dimensional image as

$$T_1(P_{mn}) = T_1'(P_{mn}) = 2P_{mn}^2, \quad 0 \leqslant P_{mn} \leqslant \tfrac{1}{2},$$
$$= T''(P_{mn}) = 1 - 2(1 - P_{mn})^2, \quad \tfrac{1}{2} \leqslant P_{mn} \leqslant 1,$$
$$m = 1, 2, \ldots, M; \quad n = 1, 2, \ldots, N.$$

P_{mn} denotes the degree of brightness of the (m, n)th pixel intensity x_{mn}. P_{mn} can be obtained from x_{mn} using any S type (monotonically nondecreasing) function [12]. The INT operator $T_1(P_{mn})$ increases the contrast around a boundary (crossover points) by increasing those P_{mn} values which are above $\frac{1}{2}$ and decreasing those which are below $\frac{1}{2}$. In general, each P_{mn} may be modified to P'_{mn} to enhance the image in the property domain by a transformation T_r where

$$P'_{mn} = T_r(P_{mn}) = T_r'(P_{mn}), \quad 0 \leqslant P_{mn} \leqslant \tfrac{1}{2},$$
$$= T_r''(P_{mn}), \quad \tfrac{1}{2} \leqslant P_{mn} \leqslant 1,$$
$$r = 1, 2, \ldots.$$

The transformation function T_s is defined as successive applications of the INT operator T_1 by the recursive relationship

$$T_s(P_{mn}) = T_1\{T_{s-1}(P_{mn})\}, \quad s = 1, 2, \ldots. \qquad (1)$$

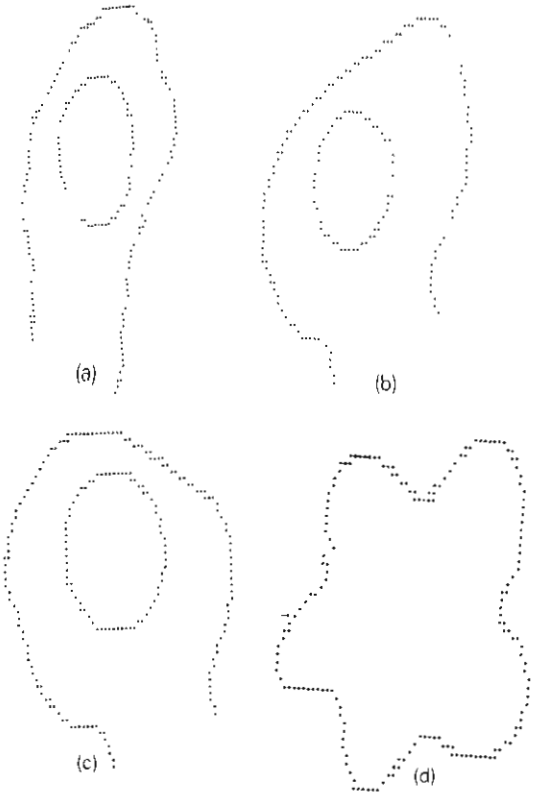

Figure 3. Contours of nuclear and cellnlar patterns of the cell images of those marked by square in Figure 1. (a) Corresponding to Fignre 1(a). (b) Corresponding to Figure 1(b). (c) Corresponding to Figure 1(c). (d) Corresponding to Fignre 1(d).

It is seen from Figure 2 that as $r \to \infty$, T_r produces a two-level (binary) image.

After the enhancement is done, the edges are extracted by

$$\text{edges} \triangleq \bigcup_m \bigcup_n x'_{mn} \qquad (2)$$

where

$$x'_{mn} = \left| x_{mn} - \min_Q \{x_{ij}\} \right|. \qquad (3)$$

Q is a set of N coordinates (i, j) which are within the circle of radius 1 centered at the point (m, n). The details of these preprocessing techniques are available in [12, 14].

Figure 3 shows the contours of nuclear and cellular patterns thus obtained corresponding to those marked by squares in Figure 1. Note that Figure 1(d) contains only the cellular contour pattern.

The edges thus produced may have in some

places more than one pixel width contour resulting in spurious wiggles. These are removed (i.e., the contours are made single pixel width) by keeping only the outer boundary pixels maintaining connectivity among them [15]. This enables us to encode the contour using the octal chain code with a view to extract the different primitives (lines and arcs) for their syntactic classification.

3.2. *Primitive extraction*

Encoding

For extracting primitives of the patterns, we have been guided by the algorithm of Pal et al. [16] where it has been possible to provide a natural way of viewing the primitives in terms of arcs with varying grades of membership from 0 to 1. Here, the contours of Figure 3 are first of all encoded into one-dimensional symbol strings using the rectangular (octal) array method. The directions of the octal codes are shown in Figure 4. An octal code is used to describe a w-pixel ($w>1$) length contour by taking the maximum of its grades of membership corresponding to 'vertical', 'horizontal' and 'oblique' lines. This approximation of using w-pixel (instead of one-pixel) length line saves computational time and storage requirement without affecting the system performance.

$\mu_V(x)$, $\mu_H(x)$ and $\mu_{ob}(x)$ representing the membership functions for vertical, horizontal and oblique lines respectively of a line segment x marking an angle θ with the horizontal line H (Figure 5) are defined as [16]

$$\mu_V(x) = 1 - |1/m_x|^{F_e}, \quad |m_x| > 1, \qquad (4)$$
$$= 0, \quad \text{otherwise},$$

$$\mu_H(x) = 1 - |m_x|^{F_e}, \quad |m_x| < 1, \qquad (5)$$
$$= 0, \quad \text{otherwise},$$

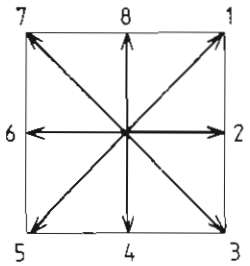

Figure 4. The directions of octal codes.

$$\mu_{ob}(x) = 1 - |(\theta - 45)/45|^{F_e}, \quad 0 < |m_x| < \infty, \qquad (6)$$
$$= 0, \quad \text{otherwise}.$$

F_e is a positive constant which controls the fuzziness in a set and $m_x = \tan\theta$.

The equations (4)–(6) are such that

$$\mu_V(x) \to 1 \quad \text{as } |\theta| \to 90°,$$

$$\mu_H(x) \to 1 \quad \text{as } |\theta| \to 0°,$$

$$\mu_{ob}(x) \to 1 \quad \text{as } |\theta| \to 45°,$$

and

$$\mu_V(x) \lesseqgtr \mu_H(x) \quad \text{as } |\theta| \lesseqgtr 45°.$$

The octal coded chains of cellular patterns for all the categories are shown for $w=3$ in Table 2.

Segmentation and contour description

The next task before extraction of primitives and description of contours is the process of segmentation of the octal coded strings. Splitting up of a chain is dependent on the constant increase/decrease in code values. For extracting an arc, the string is segmented at a position whenever a decrease/increase after constant increase/decrease in values of codes is found [16]. Again, if the number of codes between two successive changes exceeds a prespecified limit, a straight line is said to exist between two curves. In the case of a closed curve (as in the case of Figure 3(d)), a provision is kept for increasing the length of the chain by adding first two starting codes to the tail of the string. This enables one to take the continuity of the chain into account in order to reflect its proper segmentation [16]. The flowchart for segmenting a chain is available in [11, 16].

After segmentation one needs to provide a measure of curvature along with direction of the different arcs and also to measure the length of lines in order to extract the primitives. The degree

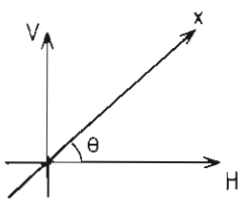

Figure 5. Membership function for vertical and horizontal lines.

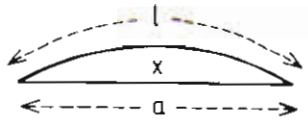

Figure 6. Membership function for arc.

of 'arcness' of a line segment x is obtained using the function [16]

$$\mu_{\text{arc}}(x) = (1 - a/l)^{F_e}. \tag{7}$$

a is the length of the line joining the two extreme points of an arc x (Figure 6), l is the arc-length such that the lower the ratio a/l is, the higher is the degree of 'arcness'.

For example, consider a sequence of codes

5 6 6 7

denoting an arc x. For computing its l note that if a code represents an oblique line, the corresponding increase in arc-length would be $\sqrt{2}$, otherwise increase is by unity. Arc diameter a is computed by measuring the resulting shifts Δm and Δn of spatial coordinates (along mth and nth axes) due to those codes in question. For the aforesaid example we have

$$\Delta m = 1 + 0 + 0 - 1 = 0,$$

$$\Delta n = -1 - 1 - 1 - 1 = -4,$$

$$a = \sqrt{\Delta m^2 + \Delta n^2} = 4,$$

$$l = 4.828,$$

$$\mu_{\text{arc}}(x) = 0.643 \quad (\text{for } F_e = 0.25).$$

Since the initial code (5) is lower than the final code (7), the sense of the curve is positive (clockwise).

Similarly, for sequences

5 6 and 5 6 7

the μ_{arc} values are respectively 0.52 and 0.682. The figures thus obtained for the different sequences agree well with our intuition as far as their degree of arcness (curvature) is concerned. Also note that the sequences like

5 5 6 6 7 7 and 5 5 5 6 6 6 7 7 7

have the same μ_{arc} value as obtained with the sequence 5 6 7. Similarly, the sequences 5 5 6 6 and 5 6 have the same μ_{arc} value.

The string descriptions of the cellular contours in terms of arcs of different arcness and line are shown in Table 2. Here, L, V and $\bar{V}$ denote the straight line, 'clockwise arc' and 'anticlockwise arc' respectively. The suffix of V represents the degree of arcness of the arc V and the superscript of L represents the number of line units respectively. As expected, the description of the contour in Figure 3(d) involves many 'sharp' arcs (high μ valued V) whereas the others contain mostly 'gentle' arcs together with consecutive straight line segments.

As an illustration, the positions of segmentation are shown by a comma (,) only for strings in Figure 3(d). It is to be mentioned here that the approach adopted here to define and to extract arcs with varying grades of membership is not the only way of doing this. One may change the procedure so as to result in segments with membership values different from those mentioned here.

3.3. *Syntactic classification*

After the primitive extraction is over, the next and final task is to classify them using four grammars. Here we have used the following simple alphabet of five primitives

$$V_T' = \{\alpha, \beta, l, \bar{\alpha}, \bar{\beta}\} \tag{8}$$

where

α = clockwise sharp curve with $\mu_{\text{arc}} \geqslant 0.64$,
β = clockwise gentle curve with $\mu_{\text{arc}} < 0.64$,
l = line segment with unit length.

$\bar{\alpha}$ and $\bar{\beta}$ are the anticlockwise versions of α and β respectively. The primitives α, β and l thus classified with thresholding over μ domain are shown in Figure 7. With these primitives, the patterns X (contour descriptions) in Table 2 can be represented as follows.

$$X_1 = \beta^2\bar{\beta}^2\beta\bar{\beta}\beta l^4\beta^2 l\beta^2 l\alpha l^4\bar{\beta}^4\beta, \tag{9a}$$

$$X_2 = \beta\bar{\beta}\beta l\beta^2 l\beta l^5\beta l\beta\alpha\beta^3\alpha\beta l\bar{\alpha}, \tag{9b}$$

$$X_3 = \beta\bar{\beta}\beta^4\bar{\beta}\beta l^2\beta^2 l\beta l^3\beta l\beta^2 l\bar{\alpha}, \tag{9c}$$

$$X_4 = l\bar{\alpha}\alpha^2\bar{\alpha}l\beta^3 l\beta\bar{\alpha}\beta l\beta^2\bar{\alpha}l\alpha\beta\bar{\beta}l\alpha l. \tag{9d}$$

Table 2
Encoded strings and their primitive description

Figure 3(a)	8 8 1 8 8 1 8 7 8 7 8 8 1 1 1 8 8 1 1 1 1 1 1 1 1 1 1 1 2 1 2 2 2 2 3 3 3 4 3 3 3 4 4 5 5 5 5 5 5 5 5 5 5 4 5 4 5 4 5 4 4 4 5 5
	$V_{.51}V_{.51}\bar{V}_{.52}\bar{V}_{.52}V_{.51}\bar{V}_{.49}V_{.52}L^4V_{.49}V_{.52}LV_{.52}V_{.49}LV_{.64}L^4\bar{V}_{.52}\bar{V}_{.52}\bar{V}_{.52}V_{.52}$
Figure 3(b)	7 8 7 6 6 7 7 7 7 8 7 7 8 8 8 8 8 1 1 1 1 1 1 1 1 1 1 1 1 1 2 1 1 1 2 1 2 2 3 3 3 4 3 4 3 4 3 4 5 4 4 5 5 5 5 5 4 4 3
	$V_{.52}\bar{V}_{.52}V_{.52}LV_{.52}V_{.49}LV_{.51}L^5V_{.52}LV_{.52}V_{.64}V_{.49}V_{.52}V_{.52}V_{.68}V_{.51}L\bar{V}_{.64}$
Figure 3(c)	7 8 7 6 6 6 7 7 7 8 7 8 7 8 8 7 8 8 1 1 1 1 1 1 1 2 1 2 2 2 2 2 3 3 3 3 3 3 3 3 3 3 4 4 4 4 4 5 4 5 5 5 5 4 4 3
	$V_{.52}\bar{V}_{.52}V_{.51}V_{.49}V_{.52}V_{.52}\bar{V}_{.52}V_{.51}L^2V_{.49}V_{.52}LV_{.51}L^3V_{.49}LV_{.51}V_{.52}L\bar{V}_{.64}$
Figure 3(d)	1 1, 1 8 7, 7 8 8 1, 1 1 2 2 3 3, 3 2 1, 1 1, 1 1 2, 2 2 3, 3 3 4, 4 4, 4 4 5, 5 4 3, 3 3 4 5, 5 5, 5 6, 6 6 7, 7 6 6 5, 5 5, 5 6 6 7, 7 8, 7 7 6, 6 6, 6 7 8, 1 1
	$L\bar{V}_{.68}V_{.64}V_{.68}\bar{V}_{.64}LV_{.49}V_{.51}V_{.49}LV_{.51}\bar{V}_{.68}V_{.49}LV_{.52}V_{51}\bar{V}_{.64}LV_{.64}V_{.52}\bar{V}_{.49}LV_{.68}L$

The four context free grammars used are

$$G_i = \{V'_{N_i}, V'_T, P_i, S\}, \quad i = 1, 2, 3, 4.$$

Here, V'_{N_i} and V'_T are the nonterminal and terminal vocabularies of the grammar G_i such that $V'_{N_i} \cap V'_T = \emptyset$ (empty set). P_i is a finite set of productions of the type $\psi \to \xi$ where ψ and ξ are strings over $V = V'_{N_i} \cup V'_T$, with ψ having at least one symbol of V'_{N_i}. $S \in V'_{N_i}$ is a starting symbol.

If an unknown string X representing the cellular contour of a neurosecretory cell

$$X \in L(G_i), \quad i = 1, 2, 3, 4,$$

then it is classified into class C_i. The classes C_i, $i = 1, 2, 3, 4$, are defined as follows:

C_1: normal (Figure 1(a)),
C_2: initial abnormal (Figure 1(b)),
C_3: middle abnormal (Figure 1(c)),
C_4: lethal abnormal (Figure 1(d)).

$L(G_i)$ denotes the language generated by grammar G_i.

The production rules P_i, $i = 1, 2, 3, 4$, for the four grammars taking into account all possible variations in a class are shown in Table 3. On parsing, the patterns X (equation (9)) are found to be correctly classified.

Some guidelines and practical considerations

It is seen from Figure 1 that class C_4 (lethal abnormal) is uniquely different from the other groups because of its lethality. Unlike the classes C_1, C_2 and C_3, it has only one contour which is again star-shaped. Maximum ambiguity lies between C_2 and C_3. The only distinguishing feature is that C_2 has an ascending line whereas, C_3 has descending characteristic.

Although, the patterns in class C_4 have closed contour, in practice due to the limitation of the pre-processing (digitisation, thresholding, enhancement and contour extraction) algorithms, it is quite likely that one may fail to preserve this closing property. Similar this is the case with classes C_1, C_2 and C_3 where the cellular contours might happen sometime to be closed. Again, the

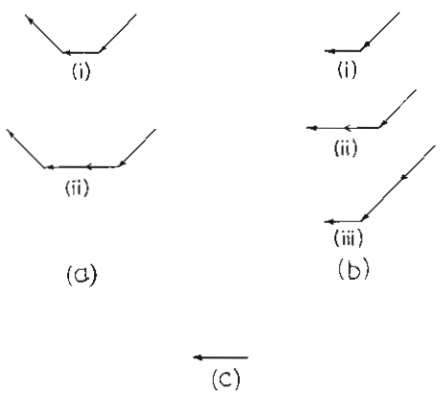

Figure 7. Different primitives. (a) Primitive α ((i), (ii) corresponding to $\mu_{arc} = 0.68$ and 0.64). (b) Primitive β ((i), (ii), (iii) corresponding to $\mu_{arc} = 0.52$, 0.51 and 0.49). (c) Primitive l.

Table 3
Production rules for classes

Class C_1	
$S \to A_1 A\beta$	$A_1 \to \beta\beta$ or 1β or $\alpha\beta$
$A \to B_1 BB_1$	$B_1 \to \bar{\beta}\bar{\beta}$ or $\bar{\beta}1$ or $\bar{\alpha}\bar{\beta}$ or $1\bar{\beta}$
$B \to C_1 CB_1$	$C_1 \to \beta\bar{\beta}\beta$ or $\beta\bar{\beta}\alpha$
$C \to 111$ or $C^1 1$	$C^1 \to D_1 D$
$D \to D_1 E$	$D_1 \to \beta\beta 1$ or $\beta\alpha$ or $\alpha 1$ or $\alpha\beta$
$E \to \alpha$	
Class C_2	
$S \to \beta A\bar{\alpha}$	$A \to \bar{\beta}B$
$B \to C^1 CC^1$	$C^1 \to \beta 1$ or 1β or $\beta\beta$
$C \to C^1 DD^1$	$D^1 \to \alpha 1$ or $\beta\alpha$ or $1\beta\beta$ or $\beta 1\beta$
$D \to 1\beta E$ or $\beta 1E$	
$E \to 1111F$	$F \to \beta 1G$ or $1\beta G$
$G \to \beta\alpha H$ or $1\alpha H$	$H \to \beta\beta$ or 1β or $\beta 1$
Class C_3	
$S \to \beta A\bar{\alpha}$	$A \to \bar{\beta}B$
$B \to C^1 CC^1$	$C^1 \to \beta 1$ or 1β or $\beta\beta$
$C \to C^1 DD^1$	$D^1 \to \alpha 1$ or $\beta\alpha$ or $1\beta\beta$ or $\beta 1\beta$
$D \to \bar{\beta}EE^1$	$E^1 \to \beta 1$ or 1β or α
$E \to E^1 F$	$F \to 1\beta G$ or $\beta 1G$
$G \to 1\beta H$ or $\beta 1H$	$H \to \beta H$
$H \to 111$	
Class C_4	
$S \to 1A1$	$A \to A_1 BA_2$
$A_1 \to \bar{\alpha}$ or $1\bar{\beta}$ or $\bar{\beta}1$	$A_2 \to \alpha$ or $\beta 1$ or 1β
$B \to A_2 A_2 C$	$C \to A_1 D1$
$D \to A_2 E\bar{\beta}$	$E \to A_2 G$
$G \to A_2 A^1 \beta$	$A^1 \to A_1 B^1 A_2$
$B^1 \to A_2 1C^1$	$C^1 \to A_2 H1$
$H \to \bar{\alpha}$	

gentle arcs may sometime be turned into a straight line. All these possible factors have been taken into consideration while formulating the grammars.

4. Conclusions and discussion

Pattern recognition techniques have been attempted here in analysing the patterns of brain neurosecretory cells. Pattern variability is found to be reflected in both size (dimension) and shape of nuclear and cellular surfaces. Various patterns of abnormalities were created by injecting thiourea. *Periplaneta americana* is taken here as an experimental tool. The algorithms used here will be applicable to higher mammalian (human too) systems. The work has therefore a great significance in biological and medical sciences. Both fuzzy and nonfuzzy set theoretic approaches have been used as a mathematical tool. Fuzzy techniques for extracting the arcs with varying grades of membership from 0 to 1 make the primitives natural. The grammars used for syntactic classification are nonfuzzy which take crisp terminals as input. Crisp primitives were obtained with thresholds over the μ_{arc} domain. Instead of nonfuzzy grammars, one can also use fuzzy and fractionally fuzzy grammars [17]. Here the aforesaid thresholding is not required and single grammar for all the classes can be used with different weights assigned to the production rules. However, this merit has to be balanced against the fact that the fuzzy grammars are not as simple as the corresponding nonfuzzy grammars used in the present work.

Acknowledgement

The authors gratefully acknowledge Sri Ashish Ghosh for doing the computational work, Sri Debasish Roy for microtome section and staining, Prof. D. Dutta Majumder for his interest in this work and Mr. J. Gupta for typing the manuscript. Authors thanks are also due to UGC for special assistance. Dr. A. Bhattacharyya is also thankful to Dr. N.B. Chatterjee for providing laboratory facilities.

References

[1] Panov, A.A. (1976). Structure of the neurosecretory system in insects. *Zool. Anz.* 196, 23–24.
[2] Raabe, M., A.A. Panov, E.D. Davydova and D. Chervin (1979). Neurosecretory products diversity iu the pars intercerebralis of insects. *Experientia* 35, 404–405.
[3] Yamasaki, T. and T. Ishii (1954). Studies on the mechanism of action of insecticides. VIII. Effects of temperature on the nerve susceptibility of DDT in the cockroach. *Botyu-Kagaku* 19, 39–46.
[4] Yamasaki, T. and T. Narahashi (1958). Nervous activity as a factor of development of dieldrin symptoms in the cockroach. *Botyu-Kagaku* 23, 47–54.
[5] Guthrie, D.M. and A.R. Tindall (1968). *The Biology of*

the Cockroach. Edward Arnold (Publishers) Ltd., London.

[6] Ulitzur, S. aud A. Poljakoff-Mayber (1963). Oxidative phesphorylation in germinating lettuce seeds. *J. Exp. Botany* 14, 95–100.

[7] Kriger, Yu.A. and I.M. Parkhomenko (1960). Protective action of thiourea. *Biofizika* 5, 278–281.

[8] Meghal, S.K. and M.C. Nath (1963). Storage of tissue thiamine and its intestinal synthesis in hypo and hyperthyroid rats, *Ann. Biochem. Exp. Med.* 23, 169–172.

[9] Rosenfeld, A. and A.C. Kak (1982). *Digital Picture Processing*. Academic Press, New York.

[10] Fu, K.S. (1982). *Syntactic Pattern Recognition and Applications*. Prentiee-Hall, Englewood Cliffs, NJ.

[11] Pal, S.K. and D. Dutta Majumder (1986). *Fuzzy Mathematical Approach to Pattern Recognition*. Wiley (Halsted), New York.

[12] Pal, S.K. and R.A. King (1981). Image enhancement using smoothing with fuzzy sets. *IEEE Trans. Syst. Man Cybern.* 11, 494–501.

[13] Zadeh, L.A. (1975). Calculus of fuzzy restrictions. In: L.A. Zadeh et al., Eds., *Fuzzy Sets and Their Applications to Cognitive and Decision Processes*. Academic Press, Loudou, 1–39.

[14] Pal, S.K. and R.A. King (1983). On edge detection of X-ray images using fuzzy set. *IEEE Trans. Pattern Anal. Machine Intell.* 5, 69–77.

[15] Pavlidis, T. (1982). *Algorithms for Graphics and Image Processing*. Springer, New York.

[16] Pal, S.K., R.A. King and A.A. Hashim (1983). Image description and primitive extraetion using fuzzy sets. *IEEE Trans. Syst. Man Cybern.* 13, 94–100.

[17] Pathak, A. and S.K. Pal (1986). Fuzzy grammars in syntactie recognition of skeletal maturity from X-rays. *IEEE Trans. Syst. Man Cybern* 16, 657–667.